PHYSICAL REVIEW A **90**, 063417 (2014)

Creation and manipulation of bound states in the continuum with lasers: Applications to cold atoms and molecules

Bimalendu Deb[1] and G. S. Agarwal[2]

[1]*Department of Materials Science, Raman Center for Atomic, Molecular and Optical Sciences, Indian Association for the Cultivation of Science, Jadavpur, Kolkata 700032, India*

[2]*Department of Physics, Oklahoma State University, Stillwater, Oklahoma 74078, USA*

(Received 27 October 2014; published 10 December 2014)

We show theoretically that it is possible to create and manipulate a pair of bound states in the continuum in ultracold atoms by two lasers in the presence of a magnetically tunable Feshbach resonance. These bound states are formed due to coherent superposition of two electronically excited molecular bound states and a quasibound state in the ground-state potential. These superposition states are decoupled from the continuum of two-atom collisional states. Hence, in the absence of other damping processes they are nondecaying. We analyze in detail the physical conditions that can lead to the formation of such states in cold collisions between atoms and discuss the possible experimental signatures of such states. An extremely narrow and asymmetric shape with a distinct minimum of the photoassociative absorption spectrum or the scattering cross section as a function of collision energy will indicate the occurrence of a bound state in the continuum (BIC). We prove that the minimum will occur at the energy at which the BIC is formed. We discuss how a BIC will be useful for efficient the creation of Feshbach molecules and manipulation of cold collisions. Experimental realizations of BIC will pave the way for a new kind of bound-bound spectroscopy in ultracold atoms.

DOI: 10.1103/PhysRevA.90.063417 PACS number(s): 34.50.Rk, 03.65.Ge, 03.65.Nk, 32.80.Qk

I. INTRODUCTION

First introduced by von Neumann and Wigner more than 80 years ago [1], a bound state in the continuum (BIC) is a counterintuitive and fundamentally profound concept. The original theoretical approach of von Neumann and Wigner has undergone extensions and modifications over the years [2–4]. In recent times, it has attracted renewed research interest [5] with prospective applications in many areas [6–10]. A BIC refers to a discreet eigenstate with an energy eigenvalue above the threshold of the continuum of a potential. The amplitude of the wave function of this state falls off in space, so the wave function is square integrable. Normally, the eigenstates of a one-particle or a multiparticle system above the continuum are infinitely extended and sinusoidal at distances larger than the range of the potential. Below the threshold, there exists a negative-energy spectrum of discrete square-integrable bound states. The idea of von Neumann and Wigner was first to assume the existence of a positive-energy square-integrable wave function with its envelop decaying in space and then to construct an appropriate potential that can support such states. Physically, a BIC occurs due to destructive interference of the outgoing Schrödinger waves scattered by the potential, creating an "unusual" trap [5] for an electron [1]. Hsu *et al.* [10] have observed trapped light, namely, a BIC of radiation modes by the destructive interference of outgoing radiations amplitudes.

Nearly 45 years after its discovery [1], Stillinger and Herrick [3] extended the idea of BIC to two-body interactions and discussed its applications in atomic and molecular physics. For two interacting particles, a BIC can be identified with a scattering resonance state with zero width. In general, a resonance at finite energies arises due to the existence of a quasibound (almost bound) state at positive energy. In the absence of any other source of dissipation, it is the coupling of the quasibound state with the continuum of scattering states that results in the finite width of the resonance. This means that a zero width of the resonance would imply decoupling of the quasibound state from the continuum of scattering states. In other words, the resonance state with zero width becomes a BIC [2,4].

Here we show that it is possible to create a BIC in cold atom-atom collisions in the presence of two photoassociation (PA) lasers near a magnetic-field-induced Feshbach resonance. Our proposed scheme is depicted in Fig. 1. The two lasers, L_1 and L_2, are tuned near the resonance of two excited molecular (bound) states, $|b_1\rangle$ and $|b_2\rangle$, respectively. We consider a magnetic Feshbach resonance of two colliding ground-state atoms with two ground-state channels, one of which one is closed and the other open. In the absence of coupling with the open channel, the closed channel is assumed to support a bound state $|b_c\rangle$. The two PA lasers couple the open-channel continuum of scattering states $|E\rangle_{\rm bare}$, with E being collision energy, and $|b_c\rangle$ to both the excited bound states. Using projector operator techniques, we analyze the resolvent operator $(z-\hat{H})^{-1}$ of the Hamiltonian operator $\hat{H}$ and thereby arrive at an effective complex Hamiltonian $\hat{H}_{\rm eff}$ of the three interacting bound states. $\hat{H}_{\rm eff}$ is non-Hermitian, and its eigenvalues are, in general, complex. However, as we will demonstrate, under appropriate physical conditions, two of the eigenvalues of the effective Hamiltonian can be made real. We establish the mathematical relations involving the parameters of our model that should hold well for the existence of the real eigenvalues. The eigenvectors corresponding to the real eigenvalues are nondecaying states and hence represent bound states in the continuum. Similar effective Hamiltonians and their eigenvalue spectrum were studied in the context of the two-photon dressed atomic continuum or autoionizing states [11–13] in the 1980s. In passing, we would like to mention that non-Hermitian Hamiltonians with real eigenvalues also arise in other areas, such as parity-time (PT) symmetric Hamiltonian systems [14,15] and the Friedrichs-Fano-Anderson model

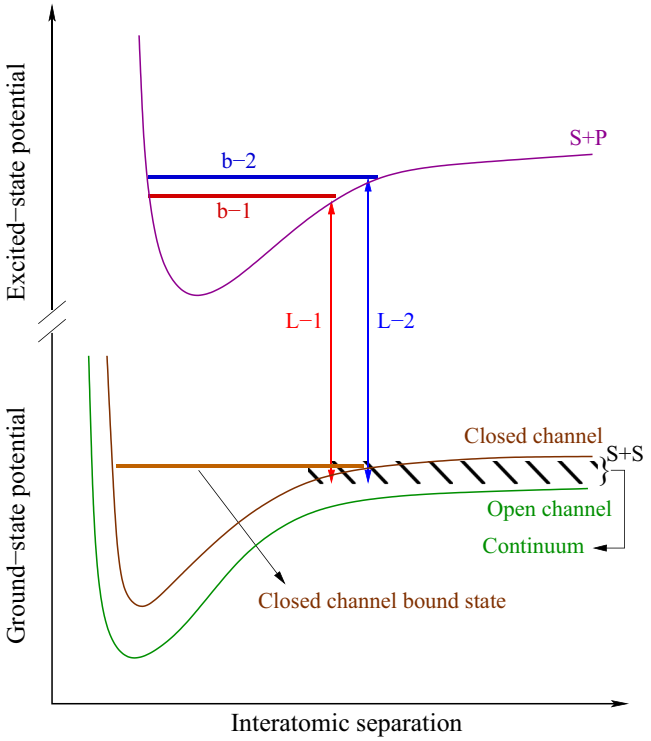

FIG. 1. (Color online) A schematic diagram for creating a BIC in ultracold atoms. Two lasers, L_1 and L_2, are used to excite PA transitions from the magnetic Feshbach-resonant collisional state of two ultracold ground-state ($S + S$) atoms to the two bound states, b_1 and b_2, respectively, in the same electronically excited molecular potential. The magnetic Feshbach resonance is considered to be a two-channel model in the electronic ground-state potentials, with the lower channel being open and the upper one being closed. In the large separation limit the ground-state channel potential corresponds to two separated $S + S$ atoms, while the excited-state potential corresponds to two separated $S + P$ atoms.

[16–18], in which a similar spectral singularity appears and can be associated with a nondecaying state in the continuum [19,20].

Here we emphasize that it is possible to detect the two predicted bound states in the continuum using two spectroscopic methods, namely, photoassociative absorption and photoassociative ionization techniques. Mathematically, a BIC in our model appears as a spectral singularity in the scattering cross section as a function of energy. The expressions for photoassociation probability of either excited bound state as well as the scattering cross section involve the inverse operator $(E - \hat{H}_{\rm eff})^{-1}$. This means that for a real eigenvalue of $\hat{H}_{\rm eff}$ the denominator of the expressions goes to zero. This leads to divergence in the scattering cross section, implying the occurrence of a resonance with zero width [2,4], that is, a BIC. However, the photoassociative absorption spectrum does not diverge for a real eigenvalue because the numerator of the expression for the spectrum also goes to zero for the real eigenvalue, canceling out the singularity of $(E - \hat{H}_{\rm eff})^{-1}$. Physically, the singularity in the scattering cross section implies that the BIC is a nondecaying state and hence is decoupled from the continuum. However, a BIC can make the transition to either of the excited bound states via BIC-bound coupling, leading to a finite probability for the absorption of a photon. Practically, spectral singularity cannot be observed in an experiment. Instead, the signature of a BIC will be manifested as an ultranarrow line in the coherent photoassociative spectrum or scattering cross section when the collision energy is tuned very close to the energy of the BIC. Usually, photoassociation is described in terms of atom loss from traps due to the formation of excited diatomic molecules decaying into two hot atoms or to a diatom that can escape from the trap. The occurrence of the bound states in the continuum in cold collisions will help us to photoassociate two atoms effectively through a bound-bound transition process which can be coherent. We show that a possible signature of a BIC in photoassociative cold collisions appears as a sharp and asymmetric line in the photoassociative absorption spectrum as a function of collision energy. Close to the sharp spikelike line, there lies a minimum which resembles the well-known Fano minimum [17] and corresponds to the energy of the BIC.

We further demonstrate that, when the intensities and the detuning parameters of L_1 and L_2 are adjusted appropriately, one of the bound states in the continuum can be reduced to a superposition of only $|b_1\rangle$ and $|b_2\rangle$, while the other BIC results from a superposition of all three bound states. We refer to the first one as A-type BIC and the second one as B-type BIC. The existence of A-type BIC can be probed by a probe laser producing the molecular ion and measuring the ion yield as a function of laser frequency. When the two continuum-bound couplings are much larger than the Feshbach resonance linewidth, the superposition coefficient of the $|b_c\rangle$ state in the B-type BIC is much larger than those of $|b_1\rangle$ and $|b_2\rangle$. Since state $|b_c\rangle$ has a magnetic moment, the B-type BIC can be probed by bound-free or bound-bound radio-frequency spectroscopy. In the case of bound-free spectra, the final state would be two free atoms, and thus, the B-type BIC can be used for controlling collisional properties of cold atoms. Furthermore, Feshbach molecules can be created by stimulating bound-bound transitions with a radio-frequency pulse at a fixed magnetic field strength. To create Feshbach molecules, the usual method uses a sudden sweep of magnetic field from the large negative to large positive scattering length sides of the Feshbach resonance. However, this sudden sweep of magnetic field leads to substantial atom loss due to an increase in kinetic energy and thereby limits the atom-molecule conversion efficiency. In contrast, since a BIC is effectively decoupled from the continuum, by creating a B-type BIC, Feshbach molecules can be produced efficiently by inducing stimulated transitions from the BIC to Feshbach molecular states with a radio-frequency pulse.

We also show that, when the coupling of the continuum to one of the bound states is turned off, one can still find one BIC, which can be identified as the familiar "dark state" made of the superposition of the two remaining bound states. Coherent population trapping occurs in this superposition state, resulting in the vanishing of the probability of the continuum of scattering states. When laser coupling to either of the excited states is turned off, the model reduces to one [21] that describes the Feshbach-resonance-induced Fano effect in photoassociation. The effective Hamiltonian approach to this model shows that the BIC appears at an energy at which

the Fano minimum occurs. This can be identified with the standard result that the population trapping occurs due to the "confluence" of coherences [22] at the Fano minimum. When the quasibound state in the ground-state potential is absent or the magnetic Feshbach resonance is turned off, the resulting effective Hamiltonian has a real eigenvalue when the corresponding eigenvector is an excited molecular dark state [23].

This paper is organized in the following way. In Secs. II and III, we present our model and its solution, respectively. We analyze in some detail how to realize our model and its application in cold atoms and molecules in Sec. IV. Finally, we discuss important conclusions of our study in Sec. V.

II. THE MODEL

The model is schematically depicted in Fig. 1. To begin with, we keep our model very general. Suppose a two-channel model is capable of describing an s-wave Feshbach resonance in a ground-state atom-atom cold collision. One of these two channels is open, and the other is closed. The closed channel is assumed to support bound state $|b_c\rangle$. The thresholds of these two ground-state channels and the binding energy of $|b_c\rangle$ are tunable by an external magnetic field. Both the bare continuum of scattering states $|E\rangle_{\rm bare}$ in the open channel, with E being the collision energy, and $|b_c\rangle$ are coupled to two bound states, $|b_1\rangle$ and $|b_2\rangle$, in an excited molecular potential by two lasers, L_1 and L_2, respectively. Suppose states $|b_1\rangle$ and $|b_2\rangle$ have the same rotational quantum number $J_1 = J_2 = 1$ but they have different vibrational quantum numbers if both of them are supported by the same adiabatic molecular potential. If they belong to different molecular potentials, their vibrational quantum numbers may be the same or different. The energy spacing between $|b_1\rangle$ and $|b_2\rangle$ is assumed to be large enough compared to the linewidths of the two lasers. Furthermore, $|b_1\rangle$ and $|b_2\rangle$ are assumed to be far below the dissociation threshold of the excited potential(s), so that the transition probability at the single-atom level is negligible.

In the rotating-wave approximation, the Hamiltonian of our mode can be expressed as $\hat{H} = \hat{H}_0 + \hat{V}$, where

$$\hat{H}_0 = \sum_n (E_n - \hbar\omega_{L_n})|b_n\rangle\langle b_n| + E_0|b_c\rangle\langle b_c| + \int E' dE' |E'\rangle_{\rm bare\ bare}\langle E'|, \tag{1}$$

$$\hat{V} = \sum_n \int dE' \Lambda_n(E')|b_n\rangle_{\rm\ bare}\langle E'| + \int dE' V_{E'}|b_c\rangle_{\rm\ bare}\langle E'| + \sum_n \hbar\Omega_n|b_n\rangle\langle b_c| + {\rm c.c.} \tag{2}$$

E_n is the binding energy of the nth excited molecular state $|b_n\rangle$, ω_{L_n} denotes the frequency of the L_n laser, E_c is the energy of the closed-channel bound state $|b_c\rangle$, and $|E'\rangle_{\rm bare}$ is the bare continuum of the scattering state with energy E'. Note that all the energies are measured from the open-channel threshold unless stated otherwise. Here $\Lambda_n(E)$ is the dipole matrix element of the transition $|E\rangle_{\rm bare} \to |b_n\rangle$, V_E is the coupling between the closed-channel bound state $|b_c\rangle$ and the open-channel scattering state $|E\rangle_{\rm bare}$, and Ω_n is the Rabi frequency between $|b_n\rangle$ and $|b_c\rangle$. The magnetic Feshbach resonance linewidth is $\Gamma_f = 2\pi|V_E|^2$.

To study BIC, we analyze the resolvent operator $G(z) = (z - \hat{H})^{-1}$ and introduce the projection operators

$$P = |b_c\rangle\langle b_c| + \sum_{n=1,2} |b_n\rangle\langle b_n|, \tag{3}$$

$$Q = 1 - P = \int dE |E\rangle_{\rm bare\ bare}\langle E|, \tag{4}$$

which satisfy the properties

$$PP = P,\ \ QQ = Q,\ \ PQ = QP = 0,\ \ P + Q = 1. \tag{5}$$

Thus, we have

$$G = G_0 + G_0\hat{V}G = \frac{1}{E - \hat{H}_0 + i\epsilon} + \frac{1}{E - \hat{H}_0 + i\epsilon}\hat{V}G. \tag{6}$$

Projecting out the bare continuum states, after some algebra given in the appendix, we obtain an effective Hamiltonian of three interacting bound states. Explicitly, this Hamiltonian is given by

$$H_{\rm eff} = H_0 + \sum_{n,n'=1,2}\left[\left(\hbar\delta_{nn'} - i\frac{\hbar\Gamma_{nn'}(E)}{2}\right)|b_n\rangle\langle b_{n'}| + \left(\delta_c - i\frac{\hbar\Gamma_f(E)}{2}\right)|b_c\rangle\langle b_c| + \sum_n \frac{\hbar\Gamma_{nf}(E)}{2}\{q_{nf} - i\}|n\rangle\langle b_c| + {\rm c.c.}\right], \tag{7}$$

where $\delta_{nn} = (E_n + \Delta_{nn}^{\rm shift})/\hbar - \omega_{L_n}$ is the detuning of the light-shifted nth excited level from the L_n laser frequency ω_{L_n}, $\delta_{nn'} = \hbar^{-1}\Delta_{nn'}^{\rm shift}$ $(n \neq n')$, with $\Delta_{nn'}^{\rm shift}$ being the real part of the quantity $\int dE' \Lambda_n^*(E')\Lambda_{n'}(E')/(E - E')$, and $\Gamma_{nn'}(E) = 2\pi\Lambda_n^*(E)\Lambda_{n'}(E)$. Here $\delta_c = \hbar^{-1}[E_c(B) + \Delta_f^{\rm shift} - E_{th}(B)]r$ is the detuning of the shifted closed-channel bound-state level from the threshold E_{th} of the open channel. Note that δ_c is a function of the applied magnetic field B due to the dependence of E_c and E_{th} on B. $\Delta_f^{\rm shift} = \mathcal{P}\int dE' |V_{E'}|^2/(E - E')$, where $\mathcal{P}$ stands for Cauchy's principal value, is the shift due to magnetic coupling $V_{E'}$ between $|b_c\rangle$ and $|E'\rangle_{\rm bare}$. q_{nf} is the well-known Fano-Feshbach asymmetry parameter defined by

$$q_{nf} = \frac{\delta_{nf}^{\rm shift} + \Omega_n}{\Gamma_{nf}/2}, \tag{8}$$

where Ω_n is the Rabi frequency for transition $|b_c\rangle \leftrightarrow |b_n\rangle$ and

$$\delta_{nf}^{\rm shift} = \hbar^{-1}\mathcal{P}\int dE' \Lambda_n^*(E')V_{E'}/(E - E') \tag{9}$$

is a frequency shift of the $|b_c\rangle \leftrightarrow |b_n\rangle$ transition frequency due to the indirect coupling of the two bound states via the continuum. Here $\Gamma_{nf} = 2\pi\hbar^{-1}\Lambda_n^*(E)V_E$. For energy E near the threshold of the continuum, the region $E' > E$ of the above integrand contributes more strongly [24]. As a result, $\delta_{nf}^{\rm shift}$ will be negative at low energy. Since Ω_n is positive, the sign of q_{nf} depends on the relative strength between $|\delta_{nf}^{\rm shift}|$ and Ω_n. Since

the magnetic coupling $V_{E'}$ is determined by the hyperfine spin coupling between the closed and the open channels, its value depends on the specific atomic system chosen. In contrast, the laser couplings Ω_n and $\delta_{nf}^{\rm shift}$ depend on which bound state $|b_n\rangle$ is chosen for the laser to be tuned to, in accordance with the Franck-Condon principle of molecular spectroscopy. Thus, it is possible to alter the sign and magnitude of the Fano-Feshbach asymmetry parameter in our model through the selectivity of the excited molecular bound states. Since, in molecular excited states, there are a host of vibrational levels in different molecular symmetries that can be accessed by PA, there is a lot of flexibility in choosing the excited bound states in our model. We will discuss this point further in Sec. IV.

In the absence of the lasers fields, the magnetic-field-dependent resonant scattering phase shift η_r and the s-wave scattering length a_s are given by

$$-\cot\eta_r = \frac{E-\tilde{E}_c}{\hbar\Gamma_f/2}. \tag{10}$$

$\tilde{E}_c = E_c + \Delta_f^{\rm shift}$ is the shifted energy of $|b_c\rangle$, and k is the wave number related to the collision energy $E = \hbar^2k^2/2\mu$, with μ being the reduced mass of the two colliding atoms. When E_c lies far above the open-channel threshold and the energy dependence of Γ_f near $E = E_c$ is weak, the Feshbach resonance linewidth Γ_f is given by its value at $E = E_c$ [25]. If the coupling V_E between the closed-channel bound state and the open-channel continuum state primarily occurs at large separations where the continuum state attains its asymptotic form, then in the limit $k \to 0$, $\Gamma_f/2 \simeq kG_f$, where G_f is a constant with the dimensions L s^{-1}. In this case we have $-\cot\eta_r \simeq \frac{1}{ka_s} + \frac{1}{2}r_0k$, where r_0 is the effective range of the open-channel ground-state potential, which is related to $\tilde{E}_c$ and G_f by $\frac{1}{a_s} = \frac{-\tilde{E}_c}{\hbar G_f}$ and $r_0 = \frac{\hbar}{\mu G_f}$, respectively. This means that the magnetic-field-dependent detuning $\delta_c(B) = -G_f/a_s$. When $\tilde{E}_c > 0$, a_s is negative, and $|b_c\rangle$ lies above the threshold of the open channel; hence, $|b_c\rangle$ is a quasibound state. In contrast, when $\tilde{E}_c < 0$, $|b_c\rangle$ is a true bound state (Feshbach molecular state), and the scattering length is positive. Later, we will show that by forming a BIC with a large scattering length, the BIC can be converted into a Feshbach molecule by stimulated radio-frequency spectroscopy.

As long as E_c is finite, one can define the resonant phase shift by Eq. (10). However, as E_c approaches the open-channel threshold ($E = 0$), $\Delta_f^{\rm shift}$ approaches a constant value, and the validity of Eq. (10) may break down [25]. This problem can be solved by using a threshold-insensitive parametrization of Γ_f [25]. It is possible to define a threshold-insensitive resonant linewidth $\tilde{\Gamma}_f$ when the coupling V_E occurs at relatively shorter separations such that Γ_f remains finite at $E = 0$.

III. THE SOLUTION

For simplicity, let us introduce the dimensionless parameters $\tilde{\delta}_n = \delta_{nn}/(\Gamma_f/2)g_n = \Gamma_{nn}/\Gamma_f$, $g_{nn'} = \Gamma_{nn'}/(\Gamma_f/2)$ ($n \neq n'$). We assume that $\delta_{12}^{\rm shift} = \delta_{21}^{\rm shift} \simeq 0$; that is, the real parts of laser-induced couplings between $|b_1\rangle$ and $|b_2\rangle$ are negligible. Assuming the two free-bound photoassociative couplings Λ_{nE} are real quantities, we have $\Lambda_{nE}V_E/|V_E|^2 = \Lambda_{nE}/V_E = \sqrt{g_n}$. Under these conditions, the effective Hamiltonian of Eq. (7) can be written in matrix form:

$$H_{\rm eff} = \frac{\hbar\Gamma_f}{2}\left[\mathbf{A} + i\mathbf{B}\right], \tag{11}$$

where

$$\mathbf{A} = \begin{pmatrix} \tilde{\delta}_1 & 0 & q_{1f}\sqrt{g_1} \\ 0 & \tilde{\delta}_2 & q_{2f}\sqrt{g_2} \\ q_{1f}\sqrt{g_1} & q_{2f}\sqrt{g_2} & -(ka_s)^{-1} \end{pmatrix} \tag{12}$$

and

$$\mathbf{B} = \begin{pmatrix} -g_1 & -g_{12} & -\sqrt{g_1} \\ -g_{21} & -g_2 & -\sqrt{g_2} \\ -\sqrt{g_1} & -\sqrt{g_2} & -1 \end{pmatrix}. \tag{13}$$

For $(ka_s)^{-1} = 0$, these matrices have the same form as Eq. (2.18) in Ref. [13]. The secular equation for the **B** matrix is $x^3 + (g_1 + g_2 + 1)x^2 = 0$, and it has two roots equal to zero and a third one equal to $-(g_1 + g_2 + 1)$. When the two eigenvectors of **B** with zero eigenvalues become simultaneous eigenvectors of **A** with real eigenvalues, we have two real roots of the effective Hamiltonian. In addition, when **A** and **B** commute, both these matrices are diagonalizable within simultaneous eigenspace, with $H_{\rm eff}$ having two real eigenvalues. The commutative condition can be easily found to be

$$q_{1f} + \tilde{\delta}_1 = q_{2f} + \tilde{\delta}_2 = q_{1f}g_1 + q_{2f}g_2 - (ka_s)^{-1}. \tag{14}$$

To evaluate the two real eigenvalues of the complex Hamiltonian $H_{\rm eff}$, we proceed in the following way. We first get an eigenvector of matrix **A** with an unknown eigenvalue λ in the form

$$X = C\begin{pmatrix} 1 \\ x_2 \\ x_3 \end{pmatrix}, \tag{15}$$

where C is a normalization constant and x_2 and x_3 are the two elements of the vector. All three quantities, C, x_2, and x_3, are functions of λ. Assuming that X is also an eigenvector of B with zero eigenvalue, the eigenvalue equation $\mathbf{B}X = 0$ leads to a quadratic equation for λ, the solutions of which are the desired eigenvalues. For $(ka_s)^{-1} = 0$, that is, for $a_s \to \infty$ or for the magnetic field tuned to the Feshbach resonance, the two real eigenvalues of $H_{\rm eff}$ are $E_\pm = \lambda_\pm\hbar\Gamma_f/2$, where

$$\lambda_\pm = \tfrac{1}{2}(\tilde{\delta}_2 - q_{1f}) \pm \tfrac{1}{2}[(\tilde{\delta}_2 + q_{1f})^2 - 4g_2q_{2f}(q_{1f} - q_{2f})]^{1/2}, \tag{16}$$

provided $(\tilde{\delta}_2 + q_{1f})^2 \geqslant 4g_2q_{2f}(q_{1f} - q_{2f})$. λ_+ and λ_- are the two eigenvalues of **A**; the corresponding eigenvectors are also the eigenvectors of **B** with both eigenvalues being zeros. The two eigenstates corresponding to these two real eigenvalues are the coherent superpositions of the three bound states and represent two bound states in the continuum. Note that the two real eigenvalues are expressed in terms of g_2, $\tilde{\delta}_2$, and the two Fano-Feshbach asymmetry parameters. However, neither of the remaining parameters, $\tilde{\delta}_1$ and g_1, can be arbitrary when $H_{\rm eff}$ has real eigenvalues. By expressing x_2, x_3, and C in terms of the set of the parameters g_2, $\tilde{\delta}_2$, q_{1f}, and q_{2f}, from the

eigenvalue equation $\mathbf{A}X = \lambda X$ one obtains

$$g_1 = \frac{(\tilde{\delta}_1 - \lambda)(\tilde{\delta}_2 - \lambda - g_2 q_{2f})}{q_{1f}(\tilde{\delta}_2 - \lambda)}, \tag{17}$$

with $\lambda \neq \tilde{\delta}_2$. Now, replacing λ by a real eigenvalue of Eq. (16), one can use the above equation to set the appropriate parameter space of g_1 and $\tilde{\delta}_1$ for which λ remains real and fixed for a fixed set of other parameters.

Let us now consider the special case in which both excited bound states belong to the same excited molecular potential with closely lying vibrational quantum numbers $1 \leqslant |v_1 - v_2| \leqslant 2$. Hence, the bound-bound Franck-Condon (FC) factors for transitions $|b_c\rangle \leftrightarrow |b_1\rangle$ and $|b_c\rangle \leftrightarrow |b_2\rangle$ will be nearly equal. Similarly, the free-bound FC factors for transitions $|E\rangle_{\text{bare}} \leftrightarrow |b_1\rangle$ and $|E\rangle_{\text{bare}} \leftrightarrow |b_2\rangle$ will also be almost equal. Since Fano asymmetry parameters q_{1f} and q_{2f} are independent of laser intensities but are dependent on these FC factors, we expect $q_{1f} \simeq q_{2f}$. The BIC condition of Eq. (14) then implies $\tilde{\delta}_1 = \tilde{\delta}_2$. Now, putting $q_{1f} = q_{2f} = q_f$, the commutativity condition implies $\tilde{\delta}_1 = \tilde{\delta}_2 = q_f(g_1 + g_2 - 1)$. Under these conditions, two real roots of the effective Hamiltonian are

$$E_A = \frac{\hbar\Gamma_f}{2}\lambda_+ = \frac{\hbar\Gamma_f}{2} q_f(g_1 + g_2 - 1), \tag{18}$$

$$E_B = \frac{\hbar\Gamma_f}{2}\lambda_- = -\frac{\hbar\Gamma_f}{2} q_f. \tag{19}$$

The BIC state corresponding to E_A is

$$|A\rangle_{\text{BIC}} = \frac{1}{\sqrt{g_1 + g_2}}[\sqrt{g_2}|b_1\rangle - \sqrt{g_1}|b_2\rangle]. \tag{20}$$

Note that this state does not mix with the closed-channel bound state $|b_c\rangle$, so this eigenvector is immune to magnetic-field tuning of the Feshbach resonance. Nevertheless, $|b_1\rangle$ and $|b_2\rangle$ remain coupled with $|b_c\rangle$ and $|E\rangle_{\text{bare}}$ due to the lasers. It is easy to see that the photoassociative transition matrix element for the interaction Hamiltonian $\hat{V}_{PA} = \sqrt{g_1}|b_1\rangle_{\text{bare}}\langle E| + \sqrt{g_2}|b_2\rangle_{\text{bare}}\langle E| + \text{c.c.}$ between $|E\rangle_{\text{bare}}$ and $|A\rangle_{\text{BIC}}$ is zero. This means that this is an excited molecular dark state that is predicted to play an important role in the suppression of photoassociative atom loss [23]. We refer to this dark state as A-type BIC. The eigenstate corresponding to the eigenvalue E_B is given by

$$|B\rangle_{\text{BIC}} = \left[\frac{1}{(g_1 + g_2)(g_1 + g_2 + 1)}\right]^{\frac{1}{2}} \times [\sqrt{g_1}|b_1\rangle + \sqrt{g_2}|b_2\rangle + (g_1 + g_2)|b_c\rangle]. \tag{21}$$

This is a superposition of all three bound states. The involvement of $|b_c\rangle$ makes this BIC dependent on the magnetic field B. We refer to this state as B-type BIC. Near the unitarity regime, $|ka_s|$ is large, and consequently, $|(ka_s)^{-1}| \ll 1$, and hence, the effect of finite $(ka_s)^{-1}$ can be taken into account perturbatively. The perturbation part of the Hamiltonian is then $V = -\frac{\hbar\Gamma_f}{2}(ka_s)^{-1}|b_c\rangle\langle b_c|$, and the first-order correction to the energy E_B is given by

$$\Delta E_B = {}_{\text{BIC}}\langle B|V|B\rangle_{\text{BIC}} = -\frac{\hbar\Gamma_f}{2}(ka_s)^{-1}\frac{g_1 + g_2}{g_1 + g_2 + 1}. \tag{22}$$

The signature of this BIC can be detected in a number of coherent spectroscopic methods, which will be discussed in the next section. For example, a BIC may manifest as a strong and narrow photoassociative absorption line.

IV. APPLICATIONS: RESULTS AND DISCUSSIONS

Before we discuss some specific applications, it is worthwhile to make some general observations about the dependence of the two real eigenvalues, E_A and E_B, on the magnetic-field tuning of the Feshbach resonance. In the zero-energy limit ($E \to 0$) and near the vicinity of the Feshbach resonance, the applied magnetic field B and the scattering length a_s are related by

$$a_s^{-1} = -a_{bg}^{-1}\frac{B - B_0}{\Delta}, \tag{23}$$

where B_0 is the resonance magnetic field at which $a_s \to \infty$ and a_{bg} is the background scattering length. Since $a_{bg}\Delta > 0$, $a_s < 0$ for $B > B_0$ and $a_s > 0$ for $B < B_0$. In the case of fermionic atoms, the $B > B_0$ ($B < B_0$) region is commonly known as the BCS (BEC) side of the resonance. The parameter range $-1.0 \leqslant (ka_s)^{-1} \leqslant 1.0$ is usually referred to as the "unitarity" regime.

Although E_A changes with the change of $(ka_s)^{-1}$, the corresponding eigenstate of Eq. (20) remains intact, so coherent population trapping (CPT) occurs in the A-type BIC that remains protected against the tuning of the magnetic field or the scattering length. In contrast, both the eigenvalue and eigenstate of the B-type BIC depends on B or a_s. For $a_s \to \infty$ and $g_1 + g_2 > 1$, as $q_f \to \pm 0$, $E_A \to \pm 0$ and $E_B \to \mp 0$, as can be inferred from expressions (18) and (19). Note that the eigenvalues of both A- and B-type BICs depend inversely on ka_s.

A. Detection of a BIC via photoassociation

Modifications of the photoassociation probability as a result of the formation of a BIC can be ascertained by making use of isometric and invertible Møller operators $\Omega_\pm$ of scattering theory. Since the atoms are in a resonant collisional state before the lasers and the magnetic field are turned on, the incoming state of the problem can be taken to be the bare continuum $|E\rangle_{\text{bare}}$. The dressed continuum state $|E+\rangle$ is given by

$$|E+\rangle = \Omega_+|E\rangle_{\text{bare}}, \tag{24}$$

where

$$\Omega_+ = 1 + G(z + i\epsilon)V. \tag{25}$$

The probability of the photoassociative transition $|E\rangle \to |b_n\rangle$ is given by

$$P_n = \int dE|\langle b_n|E+\rangle|^2. \tag{26}$$

The quantity

$$S_n(E) = |\langle b_n|E+\rangle|^2 \tag{27}$$

is the photoassociation probability per unit collision energy. Now, we have

$$\langle b_n|E+\rangle = \langle b_n|(P + Q)G(z + i\epsilon)(P + Q)V|E\rangle = \langle b_n|PG(z + i\epsilon)(P + Q)V|E\rangle_{\text{bare}}. \tag{28}$$

Using Eq. (A3) we have

$$PGQ = P(Q + GPVQ)\frac{1}{E - H_0 - VQ + i\epsilon} = PGPVQ\frac{1}{E - H_0 - VQ + i\epsilon}, \quad (29)$$

$$\langle b_n|\Omega_+|E\rangle_{\rm bare} = \langle b_n|PG(E + i\epsilon)PR(E + i\epsilon)|E\rangle_{\rm bare}, \quad (30)$$

where $R(E + i\epsilon)$ is given in Eq. (A5). Now,

$$PG(E + i\epsilon)P = (E - H_{\rm eff} + i\epsilon)^{-1} = \frac{2}{\hbar\Gamma_f}\frac{\mathscr{A}}{\mathrm{Det}[(\tilde{E} - \tilde{H}_{\rm eff}]}, \quad (31)$$

where $\tilde{E} = 2E/\hbar\Gamma_f$, $\tilde{H}_{\rm eff} = \mathbf{A} + i\mathbf{B}$, and $\mathscr{A}$ is the transpose of the cofactor matrix of $(\tilde{E} - \tilde{H}_{\rm eff})$. Thus, we have

$$\langle b_n|\Omega_+|E\rangle = \sqrt{\frac{2}{\pi\hbar\Gamma_f}}\frac{1}{\mathrm{Det}[\tilde{E} - \tilde{H}_{\rm eff}]} \times \left[\sum_{m=1,2}\mathscr{A}_{nm}\sqrt{g_m} + \mathscr{A}_{n3}\right]. \quad (32)$$

The quantity after '×' mark of the above equation, for $n = 1$ and $(ka_s)^{-1} = 0$, can be expressed as

$$\begin{aligned}&-\sqrt{g_1}[-\tilde{E}(\tilde{\delta}_2 - \tilde{E}) - g_2q_{2f}^2 - i(\tilde{\delta}_2 - \tilde{E})\\ &+ ig_2q_{2f} + ig_2q_{2f}]\\ &+\sqrt{g_2}[-q_{1f}q_{2f}\sqrt{g_1g_2} + i\sqrt{g_1g_2}(q_{1f} + q_{2f}) + i\sqrt{g_1g_2}\tilde{E}]\\ &-[-q_{1f}\sqrt{g_1}(\tilde{\delta}_2 - \tilde{E}) - ig_2\sqrt{g_1}q_{2f} + ig_2\sqrt{g_1}q_{1f}\\ &+ i\sqrt{g_1}(\tilde{\delta}_2 - \tilde{E})], \end{aligned} \quad (33)$$

the zeros of which are the roots of the quadratic equation

$$\tilde{E}(\tilde{\delta}_2 - \tilde{E}) + g_2q_{2f}^2 - q_{1f}q_{2f}g_2 + q_{1f}(\tilde{\delta}_2 - \tilde{E}) = 0. \quad (34)$$

Thus, the numerator has two zeros at

$$\tilde{E}_\pm = \tilde{\delta}_2 + \frac{1}{2}\Big[-(\tilde{\delta}_2 + q_{1f}) \pm \sqrt{(\tilde{\delta}_2 + q_{1f})^2 + 4q_{2f}g_2(q_{2f} - q_{1f})}\Big]. \quad (35)$$

It is important to note that the two zeros of the numerator are the same as the two real eigenvalues of $H_{\rm eff}$, as given in Eq. (16). This means that, although the denominator

$$\mathrm{Det}[\tilde{E} - \tilde{H}_{\rm eff}] = \sum_{i=1}^{3}(\tilde{E} - \tilde{E}_i), \quad (36)$$

where $\tilde{E}_i$ represents an eigenvalue of $\tilde{H}_{\rm eff}$, may become zero for a real eigenvalue of $\tilde{H}_{\rm eff}$, the spectrum remains finite in the limit $\tilde{E} \to E_i$ for a real eigenvalue $\tilde{E}_i \equiv \lambda_\pm$. When the real part of a complex eigenvalue is nearly equal to a real eigenvalue and the imaginary part is extremely small ($\ll\hbar\Gamma_f$), the spectrum $S(E)$ as a function of collision energy E will exhibit a Fano-like minimum and a highly prominent maximum lying close to the minimum. Experimentally, searching for such a spectral structure is possible by choosing the parameters $\tilde{\delta}_2$, g_2, q_{1f}, and q_{2f} for a zero of the numerator, but g_1 and $\tilde{\delta}_1$ are chosen such that the real part of one of the eigenvalues of $H_{\rm eff}$ is nearly equal to a zero of the numerator with the imaginary part being small. A Fano-like spectral structure with a nearby narrow spectral spike will indicate the existence of a BIC [13].

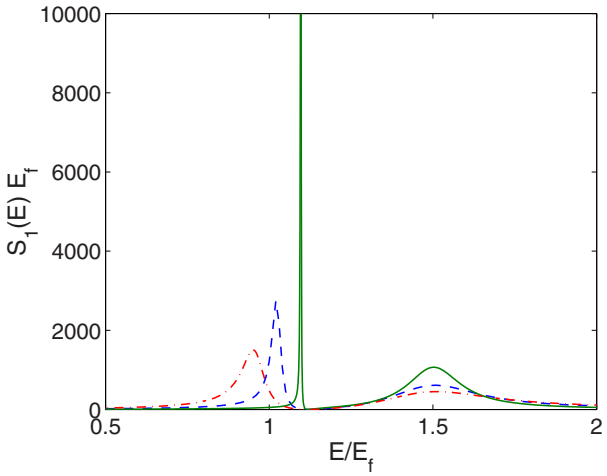

FIG. 2. (Color online) Dimensionless spectrum $S_1(E)E_f$ as a function of E/E_f (where $E_f = \hbar\Gamma_f/2$) for $g_1 = 0.25$ (solid curve), $g_1 = 0.5$ (dashed curve), and $g_1 = 0.75$ (dash-dotted curve), with $q_{1f} = -0.5$, $q_{2f} = -1.0$, $g_2 = 2.0$, $\tilde{\delta}_2 = -0.5$, and $\tilde{\delta}_1 = 1.5$. For the solid curve the three complex eigenvalues of $\tilde{H}_{\rm eff}$ are $\tilde{E}_1 = 1.0964 - 0.0010i$, $\tilde{E}_2 = 1.4989 - 0.0992i$, and $\tilde{E}_3 = -1.5953 - 3.1498i$; for the dashed curve $\tilde{E}_1 = 1.0242 - 0.0164i$, $\tilde{E}_2 = 1.4862 - 0.1653i$, and $\tilde{E}_3 = -1.5104 - 3.3184i$; for the dash-dotted curve $\tilde{E}_1 = 0.9581 - 0.0421i$, $\tilde{E}_2 = 1.4645 - 0.2111i$, and $\tilde{E}_3 = -1.4226 - 3.4968i$. When $g_1 = 0.1803$, $\tilde{E}_1$ becomes real and is equal to 1.1180, which corresponds to the minimum of the spectral lines. The spike height of the solid curve is 2.2×10^4.

Figures 2 and 3 display photoassociative absorption spectra $S_1(E)$ (which is a measure of the probability of a transition to $|b_1\rangle$) as a function of the ratio E/E_f between the energy E and $E_f = \hbar\Gamma_f/2$ for different values of g_1, with all other parameters kept fixed. The fixed parameters are chosen such that they fulfill Eq. (35). The different values of g_1 are chosen to be close to a value that is given by the condition (17) for the occurrence of a real eigenvalue $\lambda = \tilde{E}_\pm$ for the given $\tilde{\delta}_1$. The results displayed in Figs. 2 and 3 and the data mentioned in the captions clearly support our analytical results described above. The spikes in the solid curves occur due to the BIC with a real eigenvalue close to the real part of $\tilde{E}_1$. In Fig. 2, the bump near $E = 1.5E_f$ occurs due to the complex eigenvalue $\tilde{E}_2$. Note that, as can be seen from Eq. (8), the Fano-Feshbach asymmetry parameter will be positive (negative) when the Rabi frequency Ω is greater (smaller) than the magnitude $\delta_{nf}^{\rm shift}$, which is negative.

B. Possible realizations of the model

We next discuss the possibility of experimental realization of our model in ultracold atomic gases that are of current experimental interest. The discussed BIC can be realized in ultracold atoms with the currently available experimental techniques of magnetic Feshbach resonances [26] and photoassociation [27,28]. In particular, our theoretical

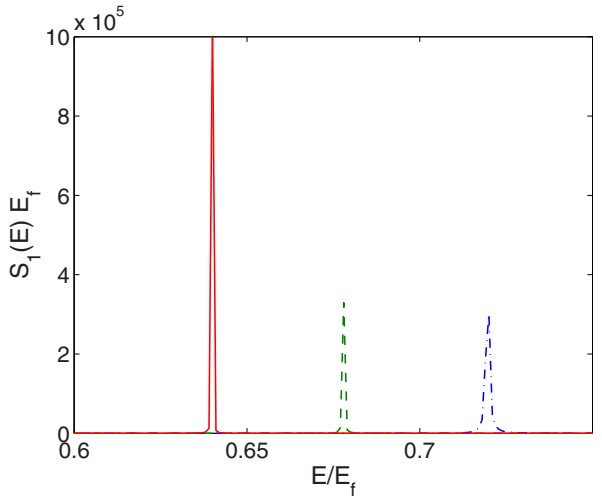

FIG. 3. (Color online) The same as Fig. 2, but for $g_1 = 5.5$ (solid curve), $g_1 = 5.0$ (dashed curve), and $g_1 = 4.5$ (dash-dotted curve) with fixed parameters $q_{1f} = 0.5$, $q_{2f} = 1.0$, $g_2 = 5.0$, $\tilde{\delta}_1 = 1.45$, and $\tilde{\delta}_2 = -1.5$. For the solid curve the eigenvalues are $\tilde{E}_1 = 0.6645 - 4.5 \times 10^{-6}i$, $\tilde{E}_2 = -2.2178 - 0.4279i$, and $\tilde{E}_3 = 1.55338 - 11.0720i$; for the dashed curve $\tilde{E}_1 = 0.7036 - 0.0002i$, $\tilde{E}_2 = -2.2165 - 0.44027i$, and $\tilde{E}_3 = 1.51292 - 10.5595i$; for the dashed-dotted curve $\tilde{E}_1 = 0.7466 - 0.0008i$, $\tilde{E}_2 = -2.2153 - 0.4534i$, and $\tilde{E}_3 = 1.4687 - 10.0457i$. For $g_1 = 5.2516$, $\tilde{E}_1$ is real and is equal to 0.6583. The spike height of the solid curve is 1.0×10^6.

proposal can be implemented in the case of experimentally observed narrow Feshbach resonances in cold alkali-metal atoms like ^{23}Na [29–34], ^{87}Rb [35–37], ^{6}Li [38,39], ^{7}Li [40,41], etc. Narrow or close-channel-dominated Feshbach resonances [26] are preferable since the lifetime of the quasibound state in such resonances will be appreciable for the lasers to excite bound-bound transitions. For the $|\chi\rangle \leftrightarrow |b_n\rangle$ bound-bound laser coupling Ω_n to be significant, one needs to choose the excited bound state $|b_n\rangle$ such that its outer turning point lies within an intermediate separation r ($20 \leqslant r \leqslant 30$) since the wave function of $|\chi\rangle$ usually peaks in this range. It is possible to find such excited bound states of alkali-metal dimers with outer turning points at such intermediate separations, and such bound state are accessible by PA transitions, which has been demonstrated in a number of experiments.

As an example, let us consider a narrow Feshbach resonance in ultracold ^{87}Rb atomic gas near a magnetic field strength of 1007.4 G [36,37] in order to realize a BIC in cold collisions. This resonance is characterized by the following parameters: zero crossing width $\Delta = 0.21$ G, background scattering length $a_{bg} = 100.5a_0$, and the difference between the magnetic moments of the closed-channel bound state $|b_c\rangle$ and the two free atoms is $\delta\mu = 2.79\mu_B$, where μ_B is the Bohr magnetron. This means the Feshbach resonance linewidth $\Gamma_f = ka_{bg}\Delta\delta\mu$, where k is the collision wave number related to the collision energy $E = \hbar^2k^2/(2\mu)$, with μ being the reduced mass of the two atoms. For $E = 50$ nK, $\Gamma_f \sim 10$ kHz. The values of parameters g_1 and g_2 used in Figs. 2 and 3 would correspond to stimulated linewidths of the order of 10 or 100 kHz. From the positions of the minimum in Figs. 2 and 3, it may be noted that a BIC will occur at sub-μK energy, requiring a Bose-Einstein condensate (BEC) of ^{87}Rb atoms in order to realize a BIC near this particular Feshbach resonance. However, the theoretical results depicted in Figs. 2 and 3 can fit into several other alkali-metal atoms for which a condensate is not essential. Moreover, different parameter regimes can be used for different alkali-metal systems. In short, our model provides a vast range of parameter space with a well-defined relationship among the various parameters for searching for a BIC in cold collisions. Before ending this section, it is worthwhile to discuss how to understand the results presented in Figs. 2 and 3 when E_c approaches the open-channel threshold since the spectra are plotted as a function of E/E_f. Typically, closed-channel bound states with E_c approaching the open-channel threshold have outer turning points at intermediate separations where the open-channel continuum wave functions cannot take asymptotic form. Thus, we can use a threshold-insensitive $E_f = \hbar\Gamma_f/2$ to scale the energy E in Figs. 2 and 3.

C. Detection of a BIC via photoassociative ionization spectroscopy

A BIC can also be detected by photoassociative ionization spectroscopy. In the BIC scheme in Fig. 1, a third laser, L_3, can be applied to excite molecular autoionization transitions $|A\rangle_{\rm BIC} \rightarrow |b_3\rangle$, where $|b_3\rangle$ represents a bound state in an excited potential that asymptotically corresponds to two atoms in $P + P$ electronic states. Since molecular state $|b_3\rangle$ is made of two doubly excited atoms, it can autoionize to produce a molecular ion. Since $|b_1\rangle$ and $|b_2\rangle$ can be chosen to be energetically close, L_3 can couple both of them to $|b_3\rangle$. Therefore, we can construct a photoassociative ionization (PAI) interaction operator

$$\hat{V}_{\rm PAI}(t) = \Omega_{31}e^{-i(\omega_{L_3}-\omega_{31})t}|b_3\rangle\langle b_1| + \Omega_{32}e^{-i(\omega_{L_3}-\omega_{32})t}|b_3\rangle\langle b_2| + \text{c.c.}, \quad (37)$$

where Ω_{31} and Ω_{32} are the Rabi frequencies for the transitions $|b_1\rangle \rightarrow |b_3\rangle$ and $|b_2\rangle \rightarrow |b_3\rangle$, respectively; ω_{L_3} is the frequency of laser L_3; and ω_{3n} is the transition frequency for the transition $|b_1\rangle \leftrightarrow |b_3\rangle$. The PAI spectrum is given by

$$S_{\rm PAI}(\omega_{L_3}) = \left| \int_0^\infty d\tau \int dE e^{-iE\tau/\hbar - \gamma\tau/2} \times \langle b_3|\hat{V}_{\rm PAI}(\tau)|E+\rangle \right|^2, \quad (38)$$

where γ is the nonradiative autoionizing linewidth of $|b_3\rangle$. Using the eigenstates $|\lambda_i\rangle$ ($i = 1,2,3$) of $H_{\rm eff}$, one can employ the identity operator $\sum_i |\lambda_i\rangle\langle\lambda_i|$ to express $\langle b_n|E+\rangle$ in terms of the $|\lambda_i\rangle$ basis:

$$\langle b_n|E+\rangle = \sum_{i=1}^{3} \frac{\langle b_n|\lambda_i\rangle\langle\lambda_i|V|E\rangle_{\rm bare}}{E - \lambda_i\hbar\Gamma_f/2 + i\epsilon}. \quad (39)$$

When BIC conditions for $q_{1f} = q_{2f} = q_f$ are fulfilled, two of the $\langle\lambda_i$ are bound states in the continuum, of which one is A type and the other is B type. For $g_1 \gg 1$ and $g_2 \gg 1$, the probability amplitudes of $|b_1\rangle$ and $|b_2\rangle$ in a B-type BIC will

be very small. Now, since the operator $\hat{V}_{\rm PAI}$ couples $|b_1\rangle$ and $|b_2\rangle$ only to $|b_3\rangle$, it is expected that, under the conditions $g_1 \gg 1$ and $g_2 \gg 1$, laser L_3 will predominantly couple an A-type BIC to $|b_3\rangle$. Thus, the PAI spectrum can be approximated as

$$S_{\rm PAI} \simeq |\,{}_{\rm BIC}\langle A|V|E\rangle_{\rm bare}|^2 \left| \frac{\Omega_{31}\sqrt{g_2}}{(\omega_{31}-\omega^A_{\rm BIC}-\omega_{L_3})+i\gamma/2} - \frac{\Omega_{32}\sqrt{g_1}}{(\omega_{32}-\omega^A_{\rm BIC}-\omega_{L_3})+i\gamma/2} \right|^2, \tag{40}$$

where $\omega^A_{\rm BIC} = E_A/\hbar$ is the eigenfrequency of the A-type BIC. Clearly, the spectrum will show a shift equal to $\omega^A_{\rm BIC}$. The spectral intensity will be suppressed (enhanced) if the quantity

$$\mathrm{Re}\left[\frac{\Omega_{31}\Omega^*_{32}\sqrt{g_1 g_2}}{(\omega_{31}-\omega^A_{\rm BIC}-\omega_{L_3}+i\gamma/2)(\omega_{32}-\omega^A_{\rm BIC}-\omega_{L_3})-i\gamma/2)} \right] \tag{41}$$

is positive (negative). Thus, one can detect the A-type BIC by PAI with a probe laser (L_3) in the presence of two PA lasers and a magnetic field under BIC conditions.

D. Controlling cold collisions with a BIC

When BIC conditions as discussed in Secs. II and III are fulfilled, the eigenstate with a real eigenvalue (i.e., BIC) effectively becomes decoupled from the bare continuum while the optical and the magnetic transitions between the continuum and the bound states remain active. As the system parameters are being tuned very close to the BIC conditions, the complex eigenvalue will tend to become real. The complex eigenvalue with a small imaginary part implies the leakage of the probability amplitude of the BIC into the continuum. This will give rise to a resonant structure with extremely narrow width [2] in the variation of the scattering cross section as a function of energy. To calculate the scattering **T** matrix, we follow the standard method of scattering theory based on Møller operators $\Omega_{\pm}$. The dressed continuum $|E+\rangle$ describes outgoing scattering waves that are influenced by laser light and the magnetic field. The part of the scattering **T**-matrix element that is modified by the two laser fields and the magnetic field is $T_{\rm field}(E) = {}_{\rm bare}\langle E|\hat{V}|E+\rangle = {}_{\rm bare}\langle E|\hat{V}\Omega_+|E\rangle_{\rm bare}$ and can be written as

$$T_{\rm field}(E) = {}_{\rm bare}\langle E|V(P+Q)G(z+i\epsilon)(P+Q)V|E\rangle_{\rm bare}. \tag{42}$$

Since ${}_{\rm bare}\langle E|VQ = 0$ and $QV|E\rangle_{\rm bare} = 0$, we have $T_{\rm field}(E) = {}_{\rm bare}\langle E|VPGPV|E\rangle_{\rm bare}$. Now, using the relation $PG(E+i\epsilon)P = (E - H_{\rm eff} + i\epsilon)^{-1}$, we can express

$$T_{\rm field}(E) = \frac{1}{\mathrm{Det}[(\tilde{E}-\tilde{H}_{\rm eff}]} \sum_{n=1}^{3} V^*_n(E) \sum_{m=1}^{3} \mathscr{A}_{nm} V_m(E), \tag{43}$$

where $V_n(E) = \Lambda_n(E)$ for $n = 1,2$ and $V_3(E) = V_E$ are the free-bound coupling constants. Assuming these coupling constants are real, we have $\Lambda_n(E) = \sqrt{\Gamma_f/\pi}\sqrt{g_n}$ and $V_E = \sqrt{\Gamma_f/\pi}$. The form of the term $\mathscr{N}_n = \sum_{m=1}^{3} \mathscr{A}_{nm} V_m(E)$ for each $n = 1,2$ is equivalent to that of the numerator of $S_n(E)$ described in Sec. IV A. We proved earlier that the numerator of $S_n(E)$ has a zero for a real eigenvalue of $H_{\rm eff}$. For $n = 3$ we have the term

$$\mathscr{N}_3 = -\frac{\Gamma_f}{2\pi}[(\tilde{E}-\tilde{\delta}_2)^2 + (\tilde{E}-\tilde{\delta}_2) \times \{\tilde{\delta}_2 - \tilde{\delta}_1 + q_{1f}g_1 + q_{2f}g_2\} + q_{2f}g_2(\tilde{\delta}_2 - \tilde{\delta}_1)]. \tag{44}$$

This expression shows that while the term $\mathscr{N}_3$ will not, in general, vanish for a real eigenvalue of $\hat{H}_{\rm eff}$, the other two terms, $\mathscr{N}_1$ and $\mathscr{N}_2$, will. $\mathscr{N}_3$ will vanish for a real eigenvalue when the commutative condition is fulfilled. This means that for an A-type or B-type BIC as discussed earlier, all three terms $\mathscr{N}_n$ ($n = 1,2,3$) in the numerator will lead to Fano-like structures with a minimum and spikelike maximum, and as the energy approaches the minimum, the spike will become narrower as in the PA absorption spectrum discussed earlier.

Ideally speaking, exactly at the BIC there will be no outgoing scattered waves. The reason is obvious: a bound state with an infinite lifetime cannot give rise to any outgoing wave. Therefore, to detect a signature of a BIC via scattering resonances, the BIC should have a small but finite width, meaning the eigenvalue should have a small imaginary part. The above analysis implies that when the system parameters are tuned closed to a BIC, the first two terms ($\mathscr{N}_1$ and $\mathscr{N}_2$) that describe the contributions from the two excited bound states will cause a Fano-like structure in the T-matrix element. Further, when the commutativity condition is fulfilled or nearly fulfilled, the A-type or B-type BIC will show up as prominent Fano-like resonances since all three terms in the numerator of Eq. (43) will contribute to the resonance structures. Thus, BIC in cold atoms can be utilized to narrow magnetic or optical Feshbach resonances or to enhance the lifetime of the resonances. Thus, after creating a BIC in cold atoms with lasers, it is possible to manipulate resonant interactions between the atoms.

E. Efficient production of Feshbach molecules using a BIC

Here we discuss how a BIC can help in the efficient production of Feshbach molecules [42] by stimulated radio-frequency spectroscopy. Note that, for $g_1 \gg 1$ and $g_2 \gg 1$, the amplitude coefficient of $|b_c\rangle$ in the B-type BIC is much greater than those of the two excited bound states. This means that when the two stimulated linewidths Γ_1 and Γ_2 are much greater than the Feshbach resonance linewidth Γ_f, by tuning the two detuning parameters to fulfill the BIC condition $\delta_1 = \delta_2 = q(\Gamma_1 + \Gamma_2 - \Gamma_f)$, one can prepare a B-type BIC with a large probability amplitude for the closed-channel bound state, which then can be converted into a Feshbach molecule by stimulated radio-frequency spectroscopy. The efficiency of the commonly used method of magnetic-field sweep for conversion of pairs of bosonic atoms into Feshbach molecules usually cannot go beyond 30%. In contrast, the efficiency of BIC-assisted Feshbach molecule formation can be close to unity. For experimental realization of BIC-assisted Feshbach molecule formation, one

can use ultracold Na atoms in the parameter regime of the experiment by Inouye *et al.* [29] and Xu *et al.* [33].

It is thus possible to suppress the atom loss in the magnetic Feshbach resonance (MFR) in Bose-Einstein condensates by creating a BIC with two lasers. This loss occurs primarily due to the disintegration of quasibound states into noncondensate atoms that can escape from the trap. To account for the loss, van Abeelen and Verhaar [31] have introduced a "local" lifetime of quasibound state $|\chi\rangle$ due to its exchange coupling to the incoming open channel at an intermediate separation. For sodium condensate, this coupling occurs at $r \leqslant 24$ and the local lifetime $\tau_0 = \frac{1}{\gamma_0} = 1.4\ \mu$s [31], where γ_0 is the width due to the coupling. By choosing the bound states $|b_1\rangle$ and $|b_2\rangle$ with outer turning points near $24a_0$ and making the bound-bound laser couplings Ω_1 and Ω_2 greater than γ_0, one can expect to suppress the atom loss to some extent. However, substantial suppression of atom loss will result when the collision energy is tuned closed to the energy of a BIC. As we analyzed earlier, the scattering T-matrix element shows a minimum when the energy becomes equal to the energy of one of the two bound states in the continuum. Since the width γ_0 is given by the energy derivative of the scattering phase shift at the energy of the quasibound state [43], in the context of our model γ_0 will correspond to the energy derivative of the phase shift at the minimum point. Thus, our model provides $\gamma_0 \simeq 0$, so atom loss in magnetic Feshbach resonances of Bose-Einstein condensates can be largely suppressed. Experimental realization of the effect of the suppression of atom loss in MFR in sodium BECs or in ultracold sodium gas is possible. Photoassociation of sodium atoms into relatively shorter ranged (outer turning points near $r \sim 24a_0$) bound states in the 1_g potential has been experimentally demonstrated [44–46] and used to create light force in PA [47] and to manipulate higher partial-wave interactions [48] via optical optical Feshbach resonance (OFR) [49].

MFR-induced atom loss in BECs is more severe partly due to bosonic stimulation unlike that in degenerate Fermi gases. Feshbach molecular dimers formed from fermionic atoms are found to be more stable [50,51] due to Pauli blocking. We therefore predict that the formation of fermionic Feshbach molecules by stimulated radio-frequency spectroscopy using a BIC will be quite efficient.

F. Two bound states coupled to the continuum

In our model we have so far considered three bound states coupled to the continuum, with one being quasibound state embedded in the ground-state continuum and the others being excited molecular states. Naturally, a question arises as to what happens to the BIC if coupling to one of the bound states is turned off. Let us first consider that one of the lasers, say L_2, is absent, that is, $g_2 = 0$. Then the effective Hamiltonian reduces to a 2×2 matrix with the second row and second column of the matrix removed. Writing the resulting 2×2 effective Hamiltonian in the form $\mathbf{A}_1 + i\mathbf{B}_1$, the matrix $\mathbf{B}_1$ has one eigenvalue equal to zero and the other one equal to $-(\hbar\Gamma_f/2)(g_1 + 1)$. Taking $E_c \simeq 0$, the condition for the existence of a real eigenvalue is $\tilde{\delta}_1 = q_{1f}g_1 - q_1$, which is also the condition for the commutativity between $\mathbf{A}_1$ and $\mathbf{B}_1$. The real eigenvalue is $-q_1$, and the corresponding eigenvector is

$$|\psi\rangle_{\rm BIC} = \frac{1}{\sqrt{\Gamma_1 + \Gamma_f}}[\sqrt{\Gamma_f}|b_1\rangle - \sqrt{\Gamma_1}|\chi\rangle]. \tag{45}$$

Now, for $E_c \neq 0$, by measuring the energy from E_c, we recover the standard result for the condition of the occurrence of Fano minimum,

$$\frac{E - E_c}{\hbar\Gamma_f/2} = -q_{1f}, \tag{46}$$

at which population trapping occurs in state $|\psi\rangle_{\rm BIC}$. This should be manifested as a prominent minimum in the scattering cross section or PA rate versus energy plot [21] as in the case of three bound states coupled to the continuum, as discussed above. In fact, a few years back, two experiments [52,53] demonstrated a minimum in the PA loss rate near the resonant value B_0 of the magnetic field that induces a Feshbach resonance. Although the spectroscopy of photoassociative atom loss or PA loss is an incoherent method, the spectral minimum observed in such an incoherent spectrum might be related to a state closely related to $|\psi\rangle_{\rm BIC}$. It is expected that in coherent PA spectroscopy or in the measurement of scattering cross sections near B_0 under the above-mentioned BIC condition, one would be able to observe the discussed minimum and an ultranarrow resonant structure as a clear signature of the occurrence of the BIC. In the experiment of Junker *et al.* [52], the quasibound state $|\chi\rangle$ is probably weakly coupled (Ω being small) to the excited bound state since the bound-state chosen was relatively long ranged, ensuring stronger free-bound Franck-Condon overlap rather than bound-bound coupling. This means that q_{1f} should be negative [21], so the minimum was expected to occur on the positive side of the scattering length, and indeed, that was the case in Ref. [52]. In contrast, the experiment by Bauer *et al.* [53] used a relatively shorter ranged excited bound state, and the minimum (although not very prominent) occurred very close to the resonant magnetic field where $a_s \to \infty$. The minimum position shows a slight shift towards the negative side of a_s as the laser is blue-detuned by about 3 MHz (the subplots in Fig. 3 of Ref. [53] should be compared). Assuming q_{1f} is positive, the BIC condition provides $\delta_1 = \omega_{b_1} - \omega_{L_1} = -q_{1f}(\Gamma_1 - \Gamma_f)$. Since in the experiment of Ref. [53] a narrow Feshbach resonance is used and a relatively strong PA laser is used, $(\Gamma_1 - \Gamma_f) > 0$. With blue detuning $(\omega_{L_1} > \omega_{b_1})$, the BIC condition will be fulfilled only if q_{1f} is positive, ensuring significant bound-bound coupling. An Autler-Townes double-peaked spectral shape will arise when the real parts of the two eigenvalues are not very far apart. If the BIC condition is maintained more precisely, it is expected that one of the peaks will be very narrow and sharp and will correspond to a BIC, while the other will be relatively broad due to the fact that the other eigenvalue is essentially complex.

We next discuss the situation when state $|\chi\rangle$ or the magnetic field is absent. Writing the resulting 2×2 matrix in the form $\mathbf{A}_2 + i\mathbf{B}_2$, one finds that $\mathbf{B}_2$ has a zero eigenvalue and the other eigenvalue is equal to $-(\Gamma_1 + \Gamma_2)$. The effective Hamiltonian has a real eigenvalue when $\delta_1 = \delta_2$. Note that δ_1 and δ_2 refer to the detuning from the light-shifted bound states. The eigenvalue is $\delta = \delta_1 = \delta_2$, and the corresponding eigenvector

is

$$|\phi\rangle_{\rm BIC} = \frac{1}{\sqrt{\Gamma_1+\Gamma_2}}[\sqrt{\Gamma_2}|b_1\rangle - \sqrt{\Gamma_1}|b_2\rangle], \tag{47}$$

which is an excited molecular dark state which has been found to be useful for making an OFR more efficient [23].

V. CONCLUSIONS

In conclusion, we have demonstrated theoretically that it is possible to create and manipulate bound states in the continuum in atom-atom cold collisions using lasers and a magnetic field, employing the currently available techniques of photoassociation and magnetic Feshbach resonance. Our model is composed of three bound states interacting with the continuum of scattering states between ground-state cold atoms. Within the framework of effective Hamiltonian methods, we eliminate the continuum and obtain an effective Hamiltonian. The eigenvectors of this effective Hamiltonian with real eigenvalues represent the bound states in the continuum. We have provided specific conditions for the occurrence of a BIC in the form of analytical expressions of the relationships between the parameters of our model. We have derived a photoassociative absorption spectrum and scattering cross sections that can exhibit signatures of a BIC as an ultranarrow asymmetric peak near a prominent minimum. The minimum occurs exactly at the energy at which the BIC occurs. We have analyzed in some detail the possible applications of a BIC in controlling cold collisions and efficient production of Feshbach molecules.

The original proposal of von Neumann and Wigner to create a BIC of a particle was through destructive quantum interference of Schrödinger's waves scattered by a specially designed potential so that no outgoing waves exist, resulting in the trapping of the particle in the continuum. The key mechanism for creating a BIC is the quantum interference, which happens not only in the scattering of waves but also in different transition pathways in atomic and molecular physics. Bound states in the continuum in our model result from the quantum interference in three possible free-bound transition pathways. In the case of two bound states interacting with the continuum, the effective Hamiltonian yields one BIC that occurs at an energy at which the Fano minimum takes place. This indicates that the BIC in our model does occur due to quantum interference in possible transition pathways. In recent times, utilization and manipulation of quantum interference effects have been essential in demonstrating a number of coherent phenomena, paving the way for emerging quantum technologies. Of late, quantum interference is being considered for manipulating ultracold collisions [54,55]. The realization of our proposed bound states in the continuum in cold collisions will open a new perspective in quantum interference phenomena with cold atoms and molecules.

APPENDIX: DERIVATION OF EFFECTIVE HAMILTONIAN

$$\hat{V}G = \hat{V}(P+Q)G = \hat{V}PG + \hat{V}QG, \tag{A1}$$

$$QG = QG_0 + \frac{Q}{E - H_0 + i\epsilon}(\hat{V}PG + \hat{V}QG), \tag{A2}$$

which leads to

$$QG = \frac{1}{E - H_0 - Q\hat{V} + i\epsilon}(Q + Q\hat{V}PG). \tag{A3}$$

Substituting (A3) in (A1) and Eq. (6), after some algebra, we get

$$PGP = \frac{1}{E - H_0 - P\hat{V}P - P\hat{V}Q\frac{1}{E-H_0-Q\hat{V}Q+i\epsilon}Q\hat{V}P},$$

which suggests that the effective Hamiltonian is

$$H_{\rm eff} = H_0 + PRP, \tag{A4}$$

where

$$R = \hat{V} + \hat{V}Q\frac{1}{E - H_0 - Q\hat{V}Q + i\epsilon}Q\hat{V}. \tag{A5}$$

Now, in the subspace of three bound states, we need to diagonalize $H_{\rm eff}$. Using Eqs. (2) and (4), we have

$$Q\hat{V}Q = 0 \tag{A6}$$

and

$$\begin{aligned}
&\hat{V}Q\frac{1}{E - H_0 - Q\hat{V}Q + i\epsilon}Q\hat{V} \\
&= \sum_{n,n'}\left[\Delta^{\rm shift}_{nn'}(E) - i\frac{\Gamma_{nn'}(E)}{2}\right]|b_n\rangle\langle b_{n'}| \\
&\quad + \left[\Delta^{\rm shift}_{f}(E) - i\frac{\Gamma_{f}(E)}{2}\right]|b_c\rangle\langle b_c| \\
&\quad + \left[\sum_n\left\{\Delta^{\rm shift}_{nf}(E) - i\frac{\Gamma_{nf}(E)}{2}\right\}|n\rangle\langle b_c| + {\rm c.c.}\right],
\end{aligned} \tag{A7}$$

where

$$\Delta^{\rm shift}_{nn'}(E) = \mathcal{P}\int dE'\frac{\Lambda_n(E')\Lambda^*_{n'}(E')}{E - E'}, \tag{A8}$$

$$\hbar\Gamma_{nn'}(E) = 2\pi\Lambda_n(E)\Lambda^*_{n'}(E), \tag{A9}$$

$$\Delta^{\rm shift}_{f}(E) = \mathcal{P}\int dE'\frac{|V_{E'}|^2}{E - E'}, \tag{A10}$$

$$\hbar\Gamma_{f}(E) = 2\pi|V_{E'}|^2, \tag{A11}$$

$$\Delta^{\rm shift}_{nf}(E) = \mathcal{P}\int dE'\frac{\Lambda_n(E')V^*_{E'}}{E - E'}, \tag{A12}$$

$$\hbar\Gamma_{nf}(E) = 2\pi\Lambda_n(E)V^*_{E}. \tag{A13}$$

Γ_f is the Feshbach resonance linewidth. Using (A6) in (A4) and (A3), one can obtain the effective Hamiltonian of Eq. (7), the matrix elements of which are given by

$$\begin{aligned}
&\langle b_n|H_{\rm eff}|b_{n'}\rangle \\
&= (E_n - \hbar\omega_{L_n})\delta_{nn'} + \Delta^{\rm shift}_{nn'}(E) - i\frac{\hbar\Gamma_{nn'}(E)}{2},
\end{aligned} \tag{A14}$$

$$\langle b_c|H_{\rm eff}|b_c\rangle = E_0 + \Delta^{\rm shift}_{f}(E) - i\frac{\hbar\Gamma_{f}(E)}{2}, \tag{A15}$$

$$\langle n|H_{\rm eff}|b_c\rangle = \Delta^{\rm shift}_{nf}(E) + \hbar\Omega_n - i\frac{\hbar\Gamma_{nf}(E)}{2}. \tag{A16}$$

[1] J. von Neumann and E. Wigner, Phys. Z. **30**, 465 (1929).
[2] L. Fonda and R. G. Newton, Ann. Phys. (NY) **10**, 490 (1960).
[3] F. H. Stillinger and D. R. Herrick, Phys. Rev. A **11**, 446 (1975).
[4] H. Friedrich and D. Wintgen, Phys. Rev. A **32**, 3231 (1985).
[5] A. G. Smart, Phys. Today **66**, 14 (2013).
[6] E. N. Bulgakov, K. N. Pichugin, A. F. Sadreev, and I. Rotter, JETP Lett. **84**, 430 (2006); A. F. Sadreev, E. N. Bulgakov, and I. Rotter, Phys. Rev. B **73**, 235342 (2006).
[7] F. Capasso *et al.*, Nature (London) **358**, 565 (1992).
[8] N. Moiseyev, Phys. Rev. Lett. **102**, 167404 (2009).
[9] Y. Plotnik, O. Peleg, F. Dreisow, M. Heinrich, S. Nolte, A. Szameit, and M. Segev, Phys. Rev. Lett. **107**, 183901 (2011).
[10] C. W. Hsu *et al.*, Nature (London) **499**, 188 (2013).
[11] A. Lami and N. K. Rahman, Phys. Rev. A **33**, 782 (1986).
[12] E. Kyröla, J. Phys. B **19**, 1437 (1986).
[13] S. L. Haan and G. S. Agarwal, Phys. Rev. A **35**, 4592 (1987).
[14] C. M. Bender and S. Boettcher, Phys. Rev. Lett. **80**, 5243 (1998).
[15] C. M. Bender, Rep. Prog. Phys. **70**, 947 (2007).
[16] K. O. Friedrichs, Commun. Pure Appl. Math. **1**, 361 (1948).
[17] U. Fano, Phys. Rev. **124**, 1866 (1961).
[18] P. W. Anderson, Phys. Rev. **124**, 41 (1961).
[19] A. Mostafazadeh, Phys. Rev. Lett. **102**, 220402 (2009).
[20] S. Longhi, Phys. Rev. B **80**, 165125 (2009).
[21] B. Deb and G. S. Agarwal, J. Phys. B **42**, 215203 (2009).
[22] K. Rzążewski and J. H. Eberly, Phys. Rev. Lett. **47**, 408 (1981).
[23] S. Saha, A. Rakshit, D. Chakraborty, A. Pal, and B. Deb, Phys. Rev. A **90**, 012701 (2014).
[24] J. L. Bohn and P. S. Julienne, Phys. Rev. A **60**, 414 (1999).
[25] H. Friedrich, *Scattering Theory*, Lecture Notes in Physics Vol. 872 (Springer, Heidelberg, 2013), Sec. 4.2.
[26] C. Chin, R. Grimm, P. S. Julienne, and E. Tiesinga, Rev. Mod. Phys. **82**, 1225 (2010).
[27] For a review of early works on photoassociation, see J. Weiner, V. S. Bagnato, S. Zilio, and P. S. Julienne, Rev. Mod. Phys. **71**, 1 (1999).
[28] For a review of ultracold photoassociation spectroscopy, see K. M. Jones, E. Tiesinga, P. D. Lett, and P. S. Julienne, Rev. Mod. Phys. **78**, 483 (2006).
[29] S. Inouye *et al.*, Nature (London) **392**, 151 (1998).
[30] J. Stenger, S. Inouye, M. R. Andrews, H.-J. Miesner, D. M. Stamper-Kurn, and W. Ketterle, Phys. Rev. Lett. **82**, 2422 (1999).
[31] F. A. van Abeelen and B. J. Verhaar, Phys. Rev. Lett. **83**, 1550 (1999).
[32] C. Samuelis, E. Tiesinga, T. Laue, M. Elbs, H. Knöckel, and E. Tiemann, Phys. Rev. A **63**, 012710 (2000).
[33] K. Xu, T. Mukaiyama, J. R. Abo-Shaeer, J. K. Chin, D. E. Miller, and W. Ketterle, Phys. Rev. Lett. **91**, 210402 (2003).
[34] T. Mukaiyama, J. R. Abo-Shaeer, K. Xu, J. K. Chin, and W. Ketterle, Phys. Rev. Lett. **92**, 180402 (2004).
[35] A. Marte, T. Volz, J. Schuster, S. Dürr, G. Rempe, E. G. M. van Kempen, and B. J. Verhaar, Phys. Rev. Lett. **89**, 283202 (2002).
[36] T. Volz, S. Dürr, S. Ernst, A. Marte, and G. Rempe, Phys. Rev. A **68**, 010702 (2003).
[37] S. Dürr, T. Volz, and G. Rempe, Phys. Rev. A **70**, 031601(R) (2004).
[38] K. E. Strecker, G. B. Partridge, and R. G. Hulet, Phys. Rev. Lett. **91**, 080406 (2003).
[39] M. W. Zwierlein, C. A. Stan, C. H. Schunck, S. M. F. Raupach, S. Gupta, Z. Hadzibabic, and W. Ketterle, Phys. Rev. Lett. **91**, 250401 (2003).
[40] K. E. Strecker, G. B. Partridge, A. G. Truscott, and R. G. Hulet, Nature (London) **417**, 150 (2002).
[41] S. E. Pollack, D. Dries, M. Junker, Y. P. Chen, T. A. Corcovilos, and R. G. Hulet, Phys. Rev. Lett. **102**, 090402 (2009).
[42] For a review on Feshbach molecules, see T. Köhler, K. Góral, and P. S. Julienne, Rev. Mod. Phys. **78**, 1311 (2006).
[43] C. J. Joachain, *Quantum Collision Theory* (North-Holland, New York, 1972).
[44] P. D. Lett, K. Helmerson, W. D. Phillips, L. P. Ratliff, S. L. Rolston, and M. E. Wagshul, Phys. Rev. Lett. **71**, 2200 (1993).
[45] P. Ratliff *et al.*, J. Chem. Phys. **101**, 2638 (1994).
[46] R. Napolitano, J. Weiner, C. J. Williams, and P. S. Julienne, Phys. Rev. Lett. **73**, 1352 (1994).
[47] E. Gomez, A. T. Black, L. D. Turner, E. Tiesinga, and P. D. Lett, Phys. Rev. A **75**, 013420 (2007).
[48] B. Deb and J. Hazra, Phys. Rev. Lett. **103**, 023201 (2009).
[49] P. O. Fedichev, Y. Kagan, G. V. Shlyapnikov, and J. T. M. Walraven, Phys. Rev. Lett. **77**, 2913 (1996).
[50] J. Cubizolles, T. Bourdel, S. J. J. M. F. Kokkelmans, G. V. Shlyapnikov, and C. Salomon, Phys. Rev. Lett. **91**, 240401 (2003).
[51] D. S. Petrov, C. Salomon, and G. V. Shlyapnikov, Phys. Rev. Lett. **93**, 090404 (2004).
[52] M. Junker, D. Dries, C. Welford, J. Hitchcock, Y. P. Chen, and R. G. Hulet, Phys. Rev. Lett. **101**, 060406 (2008).
[53] D. M. Bauer, M. L. C. Vo, G. Rempe, and S. Dürr, Nat. Phys. **5**, 339 (2009).
[54] B. Deb, J. Phys. B **43**, 085208 (2010).
[55] H. Wu and J. E. Thomas, Phys. Rev. A **86**, 063625 (2012).